

Dispersed Oil Transport Modeling Calibrated by Field-Collected Data Measuring Fluorescein Dye Dispersion

Deborah P. French-McCay, PhD¹, Christopher Mueller¹, James Payne, PhD², Eric Terrill, PhD³, Mark Otero³, Sung Yong Kim³, Melissa Carter³, Walter Nordhausen, PhD⁴, Mark Lampinen⁴, Brooke Longval¹, Melanie Schroeder¹, Kathy Jayko¹, Carter Ohlmann, PhD⁵.

¹Applied Science Associates, Inc., Narragansett, RI, USA, ²Payne Environmental Consultants, Inc, Encinitas, CA, USA, ³Scripps Institution of Oceanography, La Jolla, CA, USA, ⁴CA Department of Fish and Game, San Diego, CA, USA, ⁵U of California, Santa Barbara, CA, USA.

Abstract

Oil-spill fate and transport modeling may be used to evaluate water column hydrocarbon concentrations, potential exposure to organisms, and impacts of oil spills with and without dispersant use. Important inputs to transport modeling for such analyses are current velocities and turbulent dispersion coefficients. Fluorescein dye studies off San Diego, California, were used to calibrate an oil transport model by hindcasting movement and dispersion of dye. The oil spill model was then used to predict subsurface hydrocarbon concentrations and potential water column impacts if oil were to be dispersed into the water column under similar conditions. Field-collected data included surface currents calculated from high-frequency radar data (HF-Radar), near-surface currents from drifter measurements drogued at several depths (1m, 2m, 4m or 5m), dye concentrations measured by fluorescence, spreading and dye intensity measurements based on aerial photography, and water density profiles from CTD casts. As the dye plume quickly extended throughout an upper mixed layer (7-15m), the horizontal dye movements were better indicated by the drifters drogued to a depth near the middle of that layer than the HF-Radar, which measured surface (~top 50 cm) currents (including wind drift). Diffusion rates were estimated based on dye spreading measured by aerial photography and fluorescence-depth profiles. The model used these data as inputs, modeling of wind-forced surface water turbulence and drift as a function of wind speed and direction (based on published results of fluid dynamics studies), and Stokes law for droplet rise/sinking rates, to predict oil transport and dispersion rates within the water column. Use of such diffusion rate data in an oil fate model can provide estimates of likely dispersed oil concentrations under similar conditions, which may be used to evaluate potential impacts on water column biota. However, other conditions with different patterns of current shear (due to background currents, tidal currents, and wind stress) should be examined before these results can be generalized.

1 Introduction

1.1 Background

New federal regulations regarding response plan oil removal capacity (Caps) requirements for tank vessels and marine transportation-related facilities being developed by the US Coast Guard (USCG, 1999) are expected to result in an increased use of chemical dispersants to treat oil spills in the United States. Other

government authorities (US and internationally) are also considering more dispersant use and designating “Pre-Approval Zones” for dispersant application in the event of oil spills. The application of dispersants in those and other areas may reduce the impacts to wildlife (e.g., seabirds, sea otters) and shoreline habitats, with the potential tradeoff that the dispersed oil will cause impacts to water column organisms (French McCay and Payne, 2001; French McCay et al., 2005). Computer simulations (French McCay et al., 2006) of large dispersed oil slicks (representing the maximum potential volume that could be dispersed in one location, with area ~ 1.5 square miles) indicate that the resulting plumes may persist for several days with hydrocarbon concentrations at levels toxic to aquatic organisms. However, model inputs for such predictions are uncertain; in particular the transport and dispersion rates of oil components in the water column that determine exposure and effects on water column biota.

Oil-spill fate and transport modeling may be used to evaluate water column hydrocarbon concentrations, potential exposure to organisms (zooplankton), and the impacts of oil spills with and without use of dispersants. A number of such analyses have been performed using SIMAP (French McCay, 2003, 2004), which uses wind data, current data, and transport and weathering algorithms to calculate the mass of oil components in various environmental compartments (water surface, shoreline, water column, atmosphere, sediments, etc.), oil pathways over time (trajectories), surface oil distributions, and concentrations of the oil components in water and sediments. SIMAP’s biological effects model was then used to evaluate exposure, toxicity, and effects on each habitat and species (or species group) in the area of the spill.

Often, currents that transport oil components and organisms are estimated by a hydrodynamic model; however, observational current data, such as from high-frequency-radar (HF-Radar) systems, drifters, or current meters, may also be used. The transport models for such analyses are highly sensitive to the current velocities and turbulent dispersion coefficients input to the models, as are further calculations utilizing the transport results. In this study, we evaluate the usefulness of field-collected data from a set of fluorescein dye studies off San Diego, California, to document movement and dispersion of subsurface dissolved components (dye or dissolved hydrocarbons) over time. We analyzed HF Radar and drifter measurements of near-surface currents, dispersion coefficients based on dye spreading measurements, modeling of wind-forced surface water drift as a function of wind speed and direction (based on published results of fluid dynamics studies), and water density profiles to determine their efficacy and accuracy as inputs for modeling transport of near-surface constituents (such as dissolved hydrocarbons from naturally entrained or chemically dispersed oil). Details of these studies are in Payne et al. (2007a, b) and French-McCay et al. (2007). Payne et al. (2008, these proceedings) provide an overview of the objectives, methods, and field results.

1.2 Objectives and Approach

This paper describes (1) estimation of dispersion rates of constituents in surface water employing data collected during seven fluorescein dye experiments off San Diego, California (described in Payne et al. 2007a,b, 2008; French-McCay et al. 2007); and (2) prediction of subsurface hydrocarbon concentrations and potential

water column impacts if oil were to be dispersed into the water column under similar conditions. Small-scale transport processes need to be resolved in fate and transport modeling used in oil impact analysis in order to evaluate effects on water column biota. These small scale processes determining current velocities are complex, and as such, it is not feasible to include most of the complexities at appropriately small scales in oil spill modeling applications, both in real time and in hindcast. While three-dimensional hydrodynamic model systems have and might be developed to model the various processes and scales, a considerable location-specific effort would be required to resolve the currents in fine enough scales both spatially and temporally to accurately predict or hindcast movements of oil constituents at the scale needed to evaluate water column effects on biota. Also, there are difficulties in predicting currents with a hydrodynamic model application that does not include all the forcing functions or enough temporal detail in them, for example use of boundary conditions based on climatic means rather than date-specific patterns) to capture advection of the appropriate scale.

In modeling oil spill fate, it is common practice to use Lagrangian (particle) trajectory models to predict the transport of so-called spilletts (Lagrangian elements, LEs, etc.), which represent sub-lots of the spilled oil (e.g., Mackay et al., 1982; Spaulding et al., 1983; Spaulding, 1988; Lehr et al., 1995, 2000; French et al., 1996; Galt, 1998; Reed et al., 1999, 2000; French McCay, 2003, 2004). The current and wind fields used to force these models are either supplied by hydrodynamic and meteorological models or are interpolated/extrapolated current and wind observations. The advective movements of spilletts are typically approximated as the vector sum of the current field, an empirically-based down and cross (leeway) drift in response to wind forcing (Lange and Hufnerfuss, 1978; Allen and Plourde, 1999; Allen, 1999), a rise or sinking velocity based on Stokes law, and turbulent dispersion rate(s) modeled as a randomized movement in the horizontal and vertical dimensions. In this study we evaluated the usefulness of neutrally-buoyant dye (where rise/sinking velocity is zero) to measure turbulent dispersion rates and tested a model of wind drift.

Youssef and Spaulding (Youssef, 1993; Youssef and Spaulding 1993, 1994) developed a model of surface wind-forced current and Stokes drift, which is employed in a simplified form in SIMAP along with the option of using the even simpler approach of a constant drift rate and leeward drift angle (French McCay, 2004). The advantage of the Youssef and Spaulding model (and similar hydrodynamic models addressing these processes) is that they capture the vertical shear (decrease in speed and change in angle with increasing depth in the first few meters under the surface) of the Stokes drift which has been observed to shear subsurface plumes (French et al., 1997; Youssef and Spaulding 1993, 1994) as shown by slower movements of subsurface drifters. This vertical shear was observed in the dye experiments off San Diego (see Payne et al., 2008).

The turbulent dispersion rate (also termed eddy diffusion) parameterizes small scale motions: those turbulent eddies and motions at spatial and temporal scales smaller than the grid-cell size and time step used in the hydrodynamic model producing the advective field. Because hydrodynamic model applications need to cover large spatial domains in order to get the appropriate forcing functions correct, they typically have grid cells on the order of 1 km or more. In most oil spills, with

the exception of those where natural dispersion is extremely high and involves a large release of oil such as the *North Cape* oil spill (French McCay, 2003), the dimensions of the subsurface plumes are smaller than 1 km and very patchy (McAuliffe, 1987; French McCay, 2004; French McCay et al., 2005; NRC 2005). Even with added chemical dispersant, the plume dimensions would be expected to be small scale (French McCay and Payne, 2001), smaller than the scale captured by the advective current field typically input to oil transport models. Thus, the predicted subsurface concentrations of oil droplets and dissolved hydrocarbons from any oil spill model are dependant on the assumed small-scale turbulence parameters input to the model. These assumptions are infrequently discussed or recognized as to their importance. However, the predictions of subsurface concentrations and impacts on water column biota are largely dependent on these assumptions (see for example French McCay, 2003 where sensitivity analysis varying these assumptions was used to calibrate the SIMAP model).

The small scale turbulent motions, more simply called mixing, are caused by a number of physical forces in the surface mixed layer of the ocean: cooling and evaporation-induced convection caused by sinking denser water; wind stress transmitted to turbulence; breaking wave-induced turbulence; Langmuir circulation; wind-driven shear in the water column; etc. (Thorpe, 1995; see summary by Moum and Smyth, 2001). Most of these processes have not been modeled and many are poorly understood. Thus, empirical measurements have been used to parameterize the small scale mixing processes in many applications (Okubo, 1967; Okubo and Ozmidov, 1970). The turbulent motion is typically parameterized in Lagrangian transport models by employing a first-order random walk technique (i.e., randomizing position each time step using horizontal and vertical dispersion coefficients to scale the magnitude of the movements). Again, it is the small scale mixing processes that are of critical importance to the prediction of subsurface plume dynamics and dilution. This priority area for research is identified in the NRC (2005) report.

2. Methods

2.1 Field Experiments and Data Collection

Fluorescein dye plumes (initially 200-700 m in diameter, on average 0.2 km² in area, after all the dye was released) were tracked and sampled by a multidisciplinary team involving members from Scripps Institute of Oceanography (SIO), California Department of Fish and Game – Office of Oil Spill Prevention and Response (OSPR), the US Coast Guard (USCG), Payne Environmental Consultants, Inc. (PECI), and Applied Science Associates (ASA). These non-toxic dye plumes served in lieu of dispersed oil to represent transport and spreading of neutrally buoyant and dissolved constituents as controlled by the hydrodynamics that would influence submerged oil droplet transport. The field sampling of the plumes was conducted on seven dates during the period from 8 November 2005 through 2 November 2006 (Payne et al., 2007a,b; 2008, these proceedings).

Dye was released in the region of HF-Radar surface current coverage off Point Loma of San Diego, California, USA. Drifters drogued to specific depths were deployed to track the plume and allow their observed trajectories to be compared with HF-Radar (i.e., 25MHz Seasonde manufactured by Coastal Ocean Dynamics

Applications Radar (CODAR) Ocean Sensors, Palo Alto, CA) velocities and field observations of the dye movements. A Seabird CTD (conductivity, temperature, depth) profiling instrument was deployed to determine the mixed layer depth, an important variable for vertical dispersion. Vertical and horizontal profiles of dye concentrations, as measured by fluorescence, were made and used to determine the depth of penetration of the dye into the water column over time and horizontal dispersion rates.

Aerial photos taken from OSPR twin engine aircraft were used to track the movements and spreading of the dye over time. A Nikon digital camera fixed to the plane and pointing downward through the viewing window was used. A GPS attached to the Nikon recorded the plane's position and altitude at the time of each photograph. The depth of view of the photos appeared to be to the depth of the dye plume (order 10m), as the visual edges of the dye corresponded with the edges defined by the concentration measurements using fluorescence. Horizontal and vertical dispersion rates were estimated from measurements of the horizontal expansion of georectified images from aerial photographs and from dye concentration data as a function of depth. Details of the methods are available in Payne et al. (2007b), as summarized below.

2.2 Data Analysis

2.2.1 Photography

Dye Plume Shape Extraction Methods and Georeferencing – The aerial photographs taken during the 2006 dye experiments were processed to determine the size, position, and orientation of the dye plume over the course of each experiment. The image files were geo-referenced using ESRI's ArcView Geographic Information System (GIS) software, assuming the GPS location was at the center of the image, that the plane was perfectly level, and estimating the ground size of the image and length scale from recorded altitude at the time of the photograph. Heading information for the plane was also recorded during the experiment and used to rotate the images appropriately after they were geotransformed.

Once the images were georeferenced, image processing software (ENVI 4.3) was used to extract the dye plume from each image and create a "shape file" (i.e., a trace of the outline, in the commonly used format employed by ESRI's and other commercial GIS software systems) representing the extent of the dye plume. The software performed a "band math" operation to create a single band image, which showed the dye in sharp contrast to the surrounding water (i.e., with a sharp gradient at the dye edges to essentially zero intensity), thus indicating that most of the dye was within the dye shape. This intermediate image was then "classified" by the software to extract the initial dye shape file. The shape file was then post-processed to remove noise and calculate the area, minor axis, and major axis for the plume over the course of the experiment. Figure 1 shows the workflow.

Dye Plume Measurements and Estimation of Advection and Diffusion Rates –

The georectified images were used to describe the experiment, document spreading of the dye plume in the cross- and down-wind directions (which corresponded to either the major and minor axes in all experiments except on 22 March 2006, where the major axis was at an angle to the wind), and estimate horizontal advective

movements and turbulent dispersion (modeled as eddy diffusion) of the dye. The georectified aerial photo images (as shape files) and centroids of each image were mapped to measure advection, and compared to drifter movements and HF-Radar derived velocities (see Payne et al., 2007a,b; French-McCay et al., 2007 for details).

The georectified aerial photo images (as shape files) were used to estimate dye plume expansion and horizontal dispersion. Linear growth of the down- and cross-wind dimensions of the plume over time (t), as measured from the images, was used to estimate horizontal dispersion coefficients, D_x and D_y in the downwind (x) and crosswind (y) directions, employing the methods described in Elliott et al. (1997; see also Csanady, 1973) where dye distributions are considered Gaussian in shape and D_x and D_y are related to the variance (σ_x^2 or σ_y^2) of the Gaussian-shaped relationship between concentration and the length scale:

$$\sigma_x^2 = 2 D_x t \quad (1)$$

$$\sigma_y^2 = 2 D_y t \quad (2)$$

The values of σ_x^2 and σ_y^2 were estimated from the dimensional measurements of the dye plume images (as georectified shape files). The edges of the dye plume, as defined by the image processing above, were assumed to cover 95% of the dye below the water surface, a reasonable assumption given the steepness of the gradients observed at the edges and the results of the *in situ* fluorometry measurements of dye concentrations near the edge of the plumes (Payne et al., 2007b, 2008). Thus, the downwind length was assumed equivalent to $4\sigma_x$, and the crosswind length equivalent to $4\sigma_y$.

Following Elliott et al. (1997), trends of σ_x^2 or σ_y^2 over time were examined to determine if they were linear, such that D_x and D_y were constant in time, and so D_x and D_y could be estimated by linear regression of σ_x^2 or σ_y^2 on t . The trends were in fact linear with slopes providing estimates of $2D_x$ and $2D_y$. The regressions included intercepts, since the dye was not initially a point source, rather having an initial area and values of σ_x^2 or σ_y^2 at $t=0$.

Analogous calculations were made using the radial dimension of the plume, i.e., the square root of ($\sigma_x \sigma_y$). This would be useful for models where isotropic turbulence is assumed, i.e., where D_y is assumed equal to D_x (French-McCay et al., 2007).

2.2.2 Mixed Layer

The surface mixed layer depth and density structure are important determinants of the vertical dispersion rate. In general, the higher the slope of the density gradient with increasing water depth, the more stable the water column and the slower the dispersion. The mixed layer depth is commonly derived from CTD profile data using a threshold difference method. The depth at which density was more than 0.2 kg/m^3 from the surface value was defined as the mixed layer depth in this study.

2.2.3 Current Observations from Drifters

The drifter waypoints were mapped to show their movements relative to the dye plume. Velocity values were computed from differences in position and decomposed

into eastward (u) and northward (v) components. Velocity integration yielded the predicted movement when the drifter data were used as input to a transport model.

2.2.4 Dye Concentration Measurements

Fluorescence data were synchronized with the GPS position and analyzed to provide vertical-section views of the dye concentrations. The vertical dispersion rate was estimated from dye concentrations measured for each transect by fitting a Gaussian curve to the concentration versus depth data and its mirror image. The variance, σ_z^2 , of the dye concentration distribution was computed from:

$$\sigma_z^2 = [\sum C_z (z - z_0)^2 \Delta z] / [\sum C_z \Delta z] \quad (3)$$

An estimate of the vertical dispersion coefficient, D_z , was obtained for each transect time (t) employing the methods described in Elliott et al. (1997) where D_z is related to the variance (σ_z^2) of the Gaussian-shaped relationship between concentration and depth:

$$\sigma_z^2 = 2 D_z t \quad (4)$$

Following Elliott et al. (1997), trends of σ_z^2 over time were examined to determine if σ_z^2 increased linearly in time (i.e., D_z was constant in time), and so D_z could be estimated by linear regression of σ_z^2 on t . If D_z varied (decreased) over time, σ_z^2 versus t was fit to a power curve (French-McCay et al., 2007):

$$\sigma_z^2 = a t^m \quad (5)$$

$$D_z = (ma/2) t^{m-1} \quad (6)$$

3. Model Algorithms

3.1 Transport and Fate Model

The transport model in SIMAP (French McCay, 2003, 2004, also earlier version in French et al., 1996) and other oil spill models (Mackay et al., 1982; Spaulding et al., 1983; Spaulding, 1988; Lehr et al., 1995, 2000; Galt, 1998; Reed et al., 1999, 2000) utilize similar algorithms for calculating advective movements and turbulent dispersion. Lagrangian particles (“spillets”) are used to track the oil movements and weathering. The movements of dissolved components (i.e., dye) in three spatial dimensions over time are described by vector positions: new vector position of the spillet center is calculated from the old plus the vector sum of east-west, north-south, and vertical components of advective and diffusive velocities. Movements of oil droplets in the water column include these transport components and the rise or sinking velocity depending on droplet diameter and the density of whole oil droplets relative to the water (based on Stokes Law). Thus, the dye does not move the same as oil droplets. The dye movements are used to measure advective and diffusive velocities, to which are added vertical velocities due to oil droplet buoyancy.

The SIMAP physical fate model estimates the distribution of oil (as mass and concentrations) on the water surface, on shorelines, in the water column, and in the sediments. Processes simulated include slick spreading, evaporation of volatiles from surface oil, transport on the water surface and in the water column, randomized

dispersion, emulsification, entrainment of oil as droplets into the water column, resurfacing of larger droplets, dissolution of soluble components, volatilization from the water column, partitioning, sedimentation, stranding on shorelines, and degradation. Oil mass is tracked separately for lower-molecular-weight aromatics (1 to 3-ring aromatics), which are soluble and cause toxicity to aquatic organisms (French McCay, 2002), other volatiles, and non-volatiles. The lower molecular weight aromatics dissolve both from the surface oil slick and whole oil droplets in the water column, and they are partitioned in the water column and sediments according to equilibrium partitioning theory (French et al., 1996; French McCay, 2003, 2004).

“Whole” oil (containing non-volatiles and volatile components not yet volatilized or dissolved from the oil) is simulated as floating slicks, emulsions and/or tarballs, or as dispersed oil droplets of varying diameter (some of which may resurface). Sublots of the spilled oil are represented by Lagrangian elements (“spillets”), each characterized by mass of hydrocarbon components and water content, location, thickness, diameter, density, and viscosity. Spreading (gravitational and by transport processes), emulsification, weathering (volatilization and dissolution loss), entrainment, resurfacing, and transport processes determine the thickness, dimensions, and locations of floating oil over time. The output of the fate model includes the location, dimensions, and physical-chemical characteristics over time of each spillet representing the oil (French McCay, 2003, 2004).

Concentrations in the water column are calculated by summing mass (in subsurface Lagrangian particles) within each grid cell of grid (for example, 100 east-west cells by 100 north-south cells by 5 vertical layers) scaled each time step to just cover the dimensions of the plume. This maximizes the resolution of the contour map at each time step and reduces error caused by averaging mass over large cell volumes. Distribution of mass around the particle center is described as Gaussian in three dimensions, with one standard deviation equal to twice the diffusive distance ($2D_x t$ in the horizontal and $2D_z t$ in the vertical, where D_x is the horizontal and D_z is the vertical diffusion coefficient, and t is particle age). The plume grid edges are set at one standard deviation out from the outer-most particle. Concentrations of particulate (oil droplet) and dissolved aromatic concentrations are calculated in each cell and time step and saved to files for later viewing and calculations. These data are used by the biological effects model to evaluate exposure, toxicity, and effects.

The physical fates model has been validated with more than 20 case histories, including the *Exxon Valdez* and other large spills (French McCay, 2003, 2004; French McCay and Rowe, 2004), as well as test spills designed to verify the model’s transport algorithms (French et al., 1997).

3.2 Biological Effects Model

The biological exposure model in SIMAP estimates the area, volume, or portion of a stock or population affected by surface oil, concentrations of oil components in the water, and sediment contamination (French McCay, 2003, 2004). For wildlife (birds, mammals, and sea turtles), the number or fraction of a population suffering oil-induced effects is proportional to the water-surface area swept by oil of sufficient quantity to provide a lethal or sublethal dose to an exposed animal. The probability of exposure is related to behavior: i.e., the habitats used and percentage of the time spent in those habitats on the surface of the water.

The most toxic components of oil to water column and benthic organisms are low molecular weight compounds, which are both volatile and soluble in water, especially the aromatic compounds (National Research Council, 1985; French McCay, 2002). This is because organisms must be exposed to hydrocarbons in order for uptake to occur and aquatic biota are exposed primarily to hydrocarbons (primarily aromatics) dissolved in water. Thus, exposure and potential effects to water column and bottom-dwelling aquatic organisms are related to concentrations of dissolved aromatics in the water. Theoretically, exposure to microscopic oil droplets could also impact aquatic biota either mechanically (especially filter feeders) or as a conduit for exposure to semi-soluble aromatics (which might be taken up via the gills or digestive tract). The effects of the dissolved hydrocarbon components are additive. Other soluble compounds in oil may also add to toxic effects on biota.

Mortality is a function of duration of exposure – the longer the duration of exposure, the lower the effects concentration (see review in French McCay, 2002). At a given concentration after a certain period of time, all individuals that will die have done so. The LC50 is the lethal concentration to 50% of exposed organisms. The incipient LC50 (LC50_∞) is the asymptotic LC50 reached after infinite exposure time (or long enough that that level is approached, Figure 2). Percent mortality is a log-normal function of concentration, with the LC50 the center of the distribution.

The value of LC50_∞ ranges from 5-400 µg/L for 95% of species exposed to dissolved PAH mixtures for over 96 hrs (French McCay, 2002). The LC50_∞ for the average species is about 50 µg/L of dissolved PAH. These LC50 values have been validated with oil bioassay data (French McCay, 2002), as well as in an application of SIMAP to the *North Cape* oil spill where field and model estimates of lobster impacts were within 10% of each other (French McCay, 2003).

In SIMAP, aquatic organisms are modeled using Lagrangian particles representing schools or groups of individuals. Pre-spill densities of fish, invertebrates, and wildlife (birds, mammals, reptiles, and amphibians) are assumed evenly distributed across each habitat type defined in the application of the model. (Habitat types may be defined to resolve areas of differing density for each species, and the impact in each habitat type is then separately computed.) Mobile fish, invertebrates, and wildlife are assumed to move at random within each habitat during the simulation period. Benthic organisms either move or remain stationary on/in the bottom. Planktonic stages, such as pelagic fish eggs, larvae, and juveniles (i.e., young-of-the-year during their pelagic stage(s)), move with the currents.

Mortality of fish, invertebrates, and their eggs and larvae was computed as a function of temperature, concentration, and time of exposure. Percent mortality was estimated for each of a large number of Lagrangian particles representing organisms of a particular behavior class (i.e., planktonic, demersal, and benthic, or fish that are classed as small pelagic, large pelagic, or demersal). For each Lagrangian particle, the model evaluates exposure duration, and corrects the LC50 for time of exposure and temperature (Figure 2) to calculate mortality. The percent mortalities were summed, weighed by the area represented by each Lagrangian particle to estimate a total equivalent volume for 100% mortality. In this way, mortality was estimated on a volume basis, rather than necessitating estimates of species densities to evaluate potential impacts. In addition to the mortality estimates, the volume exceeding 1 µg/L total dissolved aromatics was used as an index for exposure for fish,

invertebrates, and plankton. The algorithms for these calculations and their validation are described in French McCay (2002, 2003, 2004).

4 Results

4.1 Wind Conditions and Mixed Layer Characteristics

Table 1 lists wind speed and direction data for the La Jolla station (LJPC1), on the shoreline 30 km north of the experimental site. Winds were generally from the west or northwest in all experiments except for that on 8 November 2005 when the wind was from the southeast. Winds were very light in the 21-22 June 2006 experiments. Winds were from a similar direction but slightly higher at the offshore weather buoy 46086, 70 km west of the experimental site.

The surface mixed layer depths during each experiment are also listed in Table 1. The dye penetrated to the depth of the mixed layer via Langmuir circulation within a half hour after release, but was not uniform in concentration over the mixed layer. Thus, the “mixed layer” was not entirely mixed in the experimental time frames. In most locations, the dye did not mix deeper than the mixed layer depth by the end of the experiment. It was apparent that the vertical dispersion rate slowed at the base of the mixed layer (as defined here), where a stronger pycnocline impeded vertical mixing. The higher degree of density stratification and shallower mixed layer observed in the June experiments would be expected, as surface heating is highest and winds are light at that time of year.

4.2 Movements of Dye and Drifters

Previous studies with the drifter found that on average the drifters typically follow the water within 1-2 cm/s (Ohlmann et al., 2007). In all seven dye studies, the drifters were initially placed within the dye (or around the edge of the plume) and were observed to remain in or close to the dye patch, with their plume following capability appearing to be governed by their drogue depth. Drifters drogued to the depth of the bulk of the dye plume stayed within the dye (see Payne et al., 2007a, b, 2008; French-McCay et al., 2007).

For experiments in 5-7 m/s winds, the drifters drogued at 4-5 m tracked the dye most accurately, whereas drifters drogued at 1-2 m moved downwind just ahead of the dye plume (e.g., 22 March 2006 experiment, Figure 3). In experiments where the surface layer was stratified and wind drift was slow and shallow (due to light winds), drifters drogued at 2 m tracked the dye most accurately, with the 4-m drifters slower than the bulk dye movements. These results were consistent with wind drift theory (Stokes drift).

4.3 Langmuir Circulation

Langmuir circulation is believed to be produced by the interaction of surface wind-forced current and Stokes drift due to waves, and cells appear if the wind is greater than a few knots (Smith, 1992; Thorpe, 2000). In the open ocean, Langmuir circulation exists in a continuum of scales from about 1-2 m to 100-200 m (Thorpe, 2000). Over time the scale evolves from smaller to larger-scale circulation (Smith, 1992), with vertical scale limited by the pycnocline depth (Thorpe, 2000) or water depth. Circulation speeds have been found to range from 1-15 cm/sec (Thorpe,

2000). The cells are unstable and reform on time scales of minutes to an hour (Thorpe, 2000).

The Langmuir circulation appears to be the process responsible for rapidly mixing the dye through the surface mixed layer (at 1 cm/s it would take 17 min to reach 10 m depth). However, the dye did not penetrate below that mixed layer during the observational period of the experiments.

4.4 Horizontal (D_x) and Vertical (D_z) Diffusion Coefficients

In all experiments but 22 March 2006 (Figure 3) and in most of the images, the major axis of the dye plume aligned with the downwind direction. Table 2 lists horizontal dispersion coefficients (D_x) calculated from the downwind and crosswind lengths of the dye plumes, as measured on the georectified images. The horizontal dispersion coefficients in the radial dimension were also calculated using the square root of the product of downwind and crosswind axis lengths. However, the horizontal dispersion coefficients vary in the downwind versus crosswind directions, indicating that horizontal dispersion is not actually isotropic (although it is often modeled that way). In the 8 November 2005 experiment (where dye images were only taken over the first hour), the dye did not spread in the crosswind axis (the slope being <0 but not significant) over the 3 images taken (after the entire dye volume was released).

The horizontal dispersion coefficients were inversely correlated with wind speed (correlation coefficients were -0.60 for downwind and -0.61 for crosswind). The highest D_x was on 21 June where winds were very light and the water column was stratified. However, while such a relationship makes sense in that wind-drift shear is greatest in the lightest winds, this data set is not large enough to determine if this is a consistent trend. The presence of current shear related to other forcing factors, and its orientation relative to wind direction, would also influence horizontal dispersion.

Vertical (D_z) dispersion coefficients were estimated (using methods outlined in Section 2.2.4) for each experimental date using dye concentration in vertical casts or transects across the dye patch (see Payne et al., 2008, for examples of dye concentration profiles). The means of the resulting coefficients on each date range from 6 to 30 cm^2/s (Table 3). However, there were only two vertical casts in the dye on 21 March 2006, making this estimate uncertain, in spite of the relatively low standard deviation (std dev). There was no trend over time in the 8 November 2005, 21 March, 22 March, 21 June and 22 June 2006 experiments. However, during the 1 and 2 November 2006 experiments, a significant trend was seen and D_z was fit to a power curve (equations 5 and 6), with results presented in Table 4. The value of D_z was order of 10 cm^2/s initially, but declined over the following 2 hours to 7 and 2 cm^2/s for 1 and 2 November 2006, respectively. The change in D_z over time may reflect evolution in Langmuir circulation cell characteristics.

4.5 Potential Impacts of Dispersed Oil Plumes

In a previous study (French-McCay et al., 2006), model estimates were made of concentrations (dissolved hydrocarbons and dispersed oil droplets) that would be expected in the surface mixed layer for the largest possible volume of oil that could be dispersed at any one location and time: the amount that could be dispersed by a single sortie of a C-130 (378.5 m^3 [100,000 gal] of light Arabian crude oil dispersed

at 80%, 45%, or 20% efficiency). Runs assuming no-dispersant use were compared to those where dispersant was applied after 8 or 16 hours of surface oil weathering, for two wind conditions: 2.5m/s (5 kts; horizontal dispersion coefficient $1 \text{ m}^2/\text{s}$; vertical dispersion coefficient $1 \text{ cm}^2/\text{s}$) and 7.5 m/s (15 kts; horizontal dispersion coefficient $10 \text{ m}^2/\text{s}$; vertical dispersion coefficient $1 \text{ cm}^2/\text{s}$). Note that these dispersion coefficients are of consistent magnitude to those measured in the dye experiments.

With 2.5m/s winds and no dispersant, the concentration plume (dissolved aromatic concentrations $>1 \text{ ppb}$) was relatively small and short-lived (hours). In 7.5 m/s winds, natural dispersion was considerable, and dispersant at 80% efficiency and the same wind conditions increased the volume affected by $>1 \text{ ppb}$ by a factor of 2-3, while decreasing bird and other wildlife impacts by a factor 4-6. In 2.5 m/s winds, dispersant use at 80% efficiency lowered wildlife impacts by a factor 2.1-2.4. Dispersant application at lower efficiencies decreased the water volume affected roughly proportionately. Variations of other model inputs resulted in smaller changes in affected volume.

In French-McCay et al. (2006), potential water-column impacts assuming a range of toxicity values characterizing 95% of species were summarized as equivalent water volumes of 100% loss. The impacted water volume for a sensitive (2.5th percentile) species was negligible in 2.5m/s of wind with no dispersant, on the order of 1-2 million m^3 in 7.5 m/s of wind for 378.5 m^3 (100,000 gal, 326.3 MT) of naturally-dispersed oil, 20-40 million m^3 in 7.5m/s of wind for 302.8 m^3 (80,000 gal, 261.0 MT) of chemically-dispersed oil (80% efficiency), and 70-200 million m^3 in 2.5m/s of wind for 302.8 m^3 of chemically-dispersed oil. The impacted water volume for a species of average sensitivity (50th percentile) was negligible in all wind conditions with no dispersant use, on the order of 0.5-0.9 million m^3 in 7.5m/s of wind for 302.8 m^3 of chemically-dispersed oil (80% efficiency), and 6-20 million m^3 in 2.5m/s of wind for 302.8 m^3 of chemically-dispersed oil (80% efficiency). Thus, the highest water column impacts were when chemical dispersant was applied under light wind conditions where dilution was relatively slow. Water volumes impacted would be much less if the oil is patchy or more spread out (because each patch would be a smaller oil volume and there would be more edge where mixing and dilution would occur), or in the cases where the efficiency of the dispersant application is less than 80% (which would be the case, as application at 80% efficiency on contiguous oil for a entire payload on a C-130 would be virtually impossible).

In the present study, similar model runs were made simulating the in-water oil concentrations after a hypothetical dispersant application using the environmental conditions at the times of the dye releases. Spill simulations were made of the March, June and November 2006 experiments using SIMAP with the following inputs:

- Near-surface current velocities as measured by the drifters placed in the dye patch;
- the radial horizontal dispersion coefficients measured from the photo images (Table 6);
- the vertical dispersion coefficients measured from fluorescence measurements (Table 7);

- restriction to the surface mixed layer as measured by the CTD casts made during each dye experiment (Payne et al., 2008); and
- Measured water temperature and salinity in the surface mixed layer.

The oil release was assumed to be a reasonable maximum volume of oil that could be dispersed in a single location: 45% of the 378.5 m³ (i.e., 170 m³ of oil) that could be treated by a full ADDS pack payload of dispersant on a C-130. A smaller volume representing 10% of 378.5 m³ (38 m³) was also run. The simulations began at the initial time of a 20-minute dispersant application, after 8-hours of weathering (properties as in French-McCay, 2006); on an optimally 100 µm-thick continuous slick of oil (assumed circular); with dispersed oil droplets set at the median size for dispersed oil based on observations by Lunel (1993a,b, 20 µm in diameter) in the surface wave-mixed layer. The model was run for 4 days, which was sufficient to disperse the oil in the water column to below acutely toxic levels for the average species (50 ppb; French McCay, 2002).

The subsurface oil concentration plume was 1-2 km in diameter and rapidly mixed through the 8-m mixed layer. Figure 4 shows the maximum concentrations at the center of the plume over time for the simulated releases of 170 m³ (45,000 gal) of oil. The horizontal dispersion coefficients ranged from 0.5-17 m²/s in the six experiments. Concentrations fell to less than 50 ppb by 5 hours after dispersant application in the 21 June experiment where the horizontal dispersion coefficient was 17 m²/s, whereas it took 74 hours for peak concentration to dilute to 50 ppb in the 22 March experiment where the horizontal dispersion coefficient was 0.5 m²/s. Figure 5 shows the maximum concentrations at the center of the plume over time for the simulated releases of 38 m³ (10,000 gal) of oil. At this lower volume, concentrations fell to less than 50 ppb by 1 hour after dispersant application in the 21 June experiment, whereas it took 8 hours for peak concentration to dilute to 50 ppb in the 22 March experiment. This is a much shorter exposure duration than for the 170 m³ (45,000 gal) release, even though the dispersed volume is still sizable. Smaller dispersed volumes would result in much lower concentrations and disperse very quickly (by a few hours).

Table 5 summarizes the water volumes and areas (for the mixed layer of 8 m deep) where species of average sensitivity (50th percentile) would be impacted (to mortality) under the conditions during each dye study. Percent loss in each affected volume was summed and divided by the mixed layer depth to calculate equivalent area of 100% mortality. For the simulated releases of 170 m³ of oil, the impacted volumes are 1-6 million m³, in an area of 0.1-0.8 km² (diameter 400-1,000 m). Note that the intensity of the peak concentration in the center of the plume, which was highest for the 22 March conditions, is not an indicator of the potential impact, as more dilution of the center of the plume can lead to a larger contaminated volume (e.g., 21 June conditions). In fact the highest impact volume occurred for the 22 June conditions, where dilution rate was in the middle of the range (horizontal dispersion coefficient 12 m²/s). Even so, the range of the estimates for impacted volume was within an order of magnitude (factor of 6). In the simulations assuming 38 m³ of oil dispersed, the impacted volume is an order of magnitude smaller, such that the area of mixed layer affected is on the order of 0.02 km² (Table 5).

The design of the modeling was to evaluate worst-case scenarios for water-column impacts, i.e., the maximum volume of oil that could be dispersed in a single

location (170 m³ of oil). Thus, the results should not be considered typical of impacts that would occur if dispersants were applied to an oil spill. Volumes and areas of water impacted would be much less if the oil was patchy or more spread out (because each patch would be a smaller volume and there would be more edge where mixing and dilution would occur). The simulations assuming 38 m³ (10,000 gal) of oil dispersed (again, in a single location) show much less impact. Thus, the water-column impact volumes and areas are conservatively high in this analysis and based on large amounts of oil dispersed in a single location.

5 Discussion and Conclusions

The drifters when drogued to a depth in the center of the vertical extent of the surface mixed layer, proved to follow the dye plumes for the temporal extent over which the studies were conducted. The results suggest they would be useful for tracking near-surface transport of oil and dissolved components as envisioned with the CA OSPR Dispersed Oil Monitoring Plan and discussed by Payne et al., (2007a, 2008).

The NRC (2005) identified estimation of turbulent dispersion coefficients (modeled as eddy diffusion) as a priority research area. Modeling results predicting hydrocarbon concentrations in the water column are highly sensitive to the assumed values for these mixing coefficients. Horizontal dispersion coefficients may be readily and accurately estimated from dye spreading as measured from aerial photographs. The photographic images are synoptic and may be made repeatedly at rapid intervals, something that cannot be done by sampling from a surface vessel. We are not aware of this approach being used in other dye studies. The results for the conditions studied indicated that the horizontal dispersion coefficient ranges from 0.1-50 m²/sec, in agreement with the literature examining these values for length scales on the order of a kilometer (e.g., Okubo, 1971; Okubo and Ozmidov, 1970). Elliott et al. (1997) performed similar dye study analyses for coastal and estuarine areas around Ireland, finding a range of 0.02-8 m²/s.

The density structure of the near-surface water is an important determinant of the dilution rate. Langmuir circulation would transport constituents into the mixed layer in a matter of minutes, as was observed in the field experiments. Vertical (D_z) dispersion coefficients were estimated for each experimental date using dye concentration in vertical casts or high-resolution fluorometer transects across the dye patch, taken after the Langmuir circulation had moved dye down and into the mixed layer. The resulting coefficients were low and typical of estimates in the literature (Okubo; Okubo and Ozmidov, 1970), reflecting minimal transport at the pycnocline beneath the mixed layer. Thus, the majority of the dilution was in the horizontal dimensions, highlighting the importance of resolving horizontal dispersion rates in order to estimate oil hydrocarbon exposure concentrations experienced by water column biota after oil is dispersed into the water column.

The SIMAP trajectory model, using the drifter velocities as current input, reproduced the trajectories of the dye (not shown), as expected, since that trajectory is controlled by the current data input and the drifters moved with the dye. The dispersion rates as calculated in this study using the aerial photo image dye dimensions could be applied to similar conditions, preferably using different parameters in the downwind and crosswind axes. The use of the radial spreading-

based horizontal dispersion coefficients should be used in models where dispersion is assumed isotropic, but this would produce a less accurate estimate of the shape of the subsurface plume. The range of wind conditions examined was not large, as these experiments were all made in fairly low wind conditions. However, the approach of using drifters and dye to estimate advection and dispersion (based on dimensional analysis of aerial photo images) could be used in actual oil spill events to evaluate impacts of dispersed oil plumes.

Use of chemical dispersants on a large volume of oil concentrated in a relatively small area could lead to toxic concentrations in the surface mixed layer of the area where oil is entrained. However, in most (if not all) cases, the floating oil being dispersed will not be in a large contiguous area of the magnitude modeled here. Volumes of water where impacts would occur would be much less if the oil is patchy or more spread out, or in the cases where the efficiency of the dispersant application is less than 45%. The latter conditions will be the norm when dispersants are applied in the field under less-than-perfect conditions, with imperfect knowledge of the location of the oil, and where oil has naturally broken up into patches and convergence zones.

The model results for offshore scenarios examined in French McCay et al. (2006), examining 378.5 m³ [100,000 gal] of light crude oil, showed that the tradeoff of decreasing wildlife impacts with dispersant use at the expense of possibly increasing water column impacts, expressed on an impacted-area basis, is very supportive of dispersant use. For the oil volume examined and assuming no dispersant use, wildlife impacts would occur on the scale of 100s km², whereas water column effects with dispersant use and as a worst case would occur on the scale of 1 km² in the upper mixed layer (10-20m deep). The exception to this support of dispersant use would be if sensitive water column biota are present in the area of the slick. Dilution would also be slower in confined water bodies than modeled here for offshore scenarios. Thus, the results and conclusions presented here apply to unconfined water bodies that are at least 10m deep.

6 Acknowledgements

Funding for this program was provided by the California Department of Fish and Game Office of Spill Prevention and Response (DFG Agreement Number P0475036 with SIO) and the NOAA/UNH Coastal Response Research Center (Grant No. NA04NOS4190063 – UNH Subcontract No. 06-084 with PECI). The findings, opinions, and recommendations expressed in this paper are those of the authors and do not necessarily reflect those of the sponsoring agencies, subagencies, or the University of New Hampshire.

We also thank the following personnel and their respective agencies for their contributions in collecting data and valuable inputs to the study: William Middleton and Andy Chen from Scripps Institution of Oceanography; Robin Lewis and Thomas Evans from the California Department of Fish and Game Office of Spill Prevention and Response (CA OSPR); BM-1 Greg L. Via, BM-1 Hector Ruiz-Santana, MK-1 Mike Maly, MSTC Butch Willoughby, and BM-2 Charles Varela from the United States Coast Guard (USCG) Pacific Strike Team; Paul Lynch and Paul Sanchez from the Marine Spill Response Corporation (MSRC); and Jan Svejkovsky and Jamie Kum of Ocean Imaging, Solana Beach, CA. We are also most grateful for the in-kind

contributions of equipment/instrumentation and sampling/observation platforms (boats and aircraft) from the USCG, MSRC, and CA OSPR. We also appreciate the careful review and input provided by anonymous reviewers and Dr. Malcolm Spaulding of the University of Rhode Island, Narragansett, RI.

7 Biography

Deborah French McCay received her bachelor's degree in Zoology from Rutgers in 1974 and her Ph.D. in Biological Oceanography from the University of Rhode Island in 1984. She is a Principal at Applied Science Associates (Narragansett, RI, USA), where she specializes in quantitative assessments and modeling of aquatic ecosystems and populations, oil and chemical transport and fates, toxicity, exposure and the bioaccumulation of pollutants by biota, along with the effects of this contamination. These models have been used for impact, risk, and natural resource damage assessments, as well as for studies of the biological systems.

8 References

- Allen, A.A., 1999. Leeway divergence. US Coast Guard Research and Development Center, Groton, CT, Report CG-D-XX-99.
- Allen, A.A. and J. V. Plourde, 1999. Review of leeway: field experience and implementation. US Coast Guard Research and Development Center, Groton, CT, Report CG-D-08-99.
- Csanady, G.T. , 1973. Turbulent Diffusion in the Environment. D. Reidel Publishing Company, Boston, 248p.
- Elliott, A.J., N. Hurford, and C.J. Penn, 1986. Shear Diffusion and the Spreading of Oil Slicks. *Marine Pollution Bulletin*, 17 (7), pp. 308-313.
- Elliott, A.J., A.G. Barr, and D. Kennan, 1997. Diffusion in Irish Coastal Waters. *Estuarine, Coastal and Shelf Science*, 44 (Supplement A), pp. 15-23.
- French, D., M. Reed, K. Jayko, S. Feng, H. Rines, S. Pavignano, T. Isaji, S. Puckett, A. Keller, F.W. French III, D. Gifford, J. McCue, G. Brown, E. MacDonald, J. Quirk, S. Natzke, R. Bishop, M. Welsh, M. Phillips and B.S. Ingram, 1996. *Final Report, The CERCLA Type A Natural Resource Damage Assessment Model for Coastal and Marine Environments (NRDAM/CME), Technical Documentation, Vol. I - V.*, Submitted to the Office of Environmental Policy and Compliance, U.S. Department of the Interior, Washington, DC, Contract No. 14-0001-91-C-11, April 1996.
- French McCay, D.P., 2002. Development and Application of an Oil Toxicity and Exposure Model, OilToxEx, *Environmental Toxicology and Chemistry*, 21:10, pp. 2080-2094.
- French McCay, D.P., 2003. Development and Application of Damage Assessment Modeling: Example Assessment for the North Cape Oil Spill. *Marine Pollution Bulletin*, 47 (9-12), pp. 341-359.
- French McCay, D.P., 2004. Oil Spill Impact Modeling: Development and Validation. *Environmental Toxicology and Chemistry*, 23 (10), pp. 2441-2456.
- French McCay, D.P. and J.R. Payne, 2001. Model of Oil Fate and Water Concentrations With and Without Application of Dispersants. In: *Proceedings of the Twenty-fourth Arctic and Marine Oil Spill Program (AMOP) Technical*

- Seminar*, Emergencies Science Division, Environment Canada, Ottawa, ON, pp. 611-645.
- French, D.P., H. Rines and P. Masciangioli, 1997. Validation of an Orimulsion Spill Fates Model Using Observations from Field Test Spills. In: *Proceedings of the Twentieth Arctic and Marine Oilspill Program (AMOP) Technical Seminar*, Emergencies Science Division, Environment Canada, Ottawa, ON, pp. 933-961.
- French McCay, D., N. Whittier, J.J. Rowe, S. Sankaranarayanan and H.-S. Kim, 2005. Use of Probabilistic Trajectory and Impact Modeling to Assess Consequences of Oil Spills with Various Response Strategies. In: *Proceedings of the 28th Arctic and Marine Oil Spill Program (AMOP) Technical Seminar*, Emergencies Science Division, Environment Canada, Ottawa, ON, Canada, pp. 253-271.
- French-McCay, D.P., J.J. Rowe, W. Nordhausen and J.R. Payne, 2006. Modeling Potential Impacts of Effective Dispersant Use on Aquatic Biota. In: *Proceedings of the 29th Arctic and Marine Oil Spill Program (AMOP) Technical Seminar*, Emergencies Science Division, Environment Canada, Ottawa, ON, Canada, pp. 855-878.
- French-McCay, D.P., C. Mueller, K. Jayko, B. Longval, M. Schroeder, J.R. Payne, E. Terrill, M. Carter, M. Otero, S. Y. Kim, W. Nordhausen, M. Lampinen, and C. Ohlmann, 2007. Evaluation of Field-Collected Data Measuring Fluorescein Dye Movements and Dispersion for Dispersed Oil Transport Modeling. In: *Proceedings of the 30th Arctic and Marine Oil Spill Program (AMOP) Technical Seminar*, Emergencies Science Division, Environment Canada, Ottawa, ON, Canada, pp.713-754.
- Galt, J.A., 1998. Uncertainty Analysis Related to Oil Spill Modeling. *Spill Science and Technology Bulletin*, 4 (4), pp. 231-238.
- Lange, P. and H. Hufnerfuss, 1978. Drift Response of Mono Molecular Slicks to Wave and Wind Action. *Journal of Physical Oceanography*, 8, pp. 142-150.
- Lehr, W.J., J.A. Galt, and R. Overstreet, 1995. Handling Uncertainty in Oil Spill Modeling. In: *Proceedings of the 18th Arctic and Marine Oil Spill Program (AMOP) Technical Seminar*, Environment Canada, pp. 759-768.
- Lehr, W.J., D. Wesley, D. Simecek-Beatty, R. Jones, G. Kachook and J. Lankford, 2000. Algorithm and Interface Modifications of the NOAA Oil Spill Behavior Model. In: *Proceedings of the 23rd Arctic and Marine Oil Spill Program (AMOP) Technical Seminar*, Vancouver, BC, Environmental Protection Service, Environment Canada, pp. 525-539.
- Lunel, T. 1993a. Dispersion: oil droplet size measurements at sea. In: *Proceedings of the Sixteenth Arctic Marine Oilspill Program (AMOP) Technical Seminar*, Emergencies Science Division, Environment Canada, Ottawa, Ontario, Canada, pp. 1023-1056.
- Lunel, T. 1993b. Dispersion: oil droplet size measurements at sea. In: *Proceedings of the 1993 Oil Spill Conference*, American Petroleum Institute, Washington, D.C., pp.794-795.
- Mackay, D, W.Y. Shiu, K. Hossain, W. Stiver, D. McCurdy and S. Peterson, 1982. Development and Calibration of an Oil Spill Behavior Model. Report No. CG-D-27-83, U.S. Coast Guard, Research and Development Center, Groton, Connecticut, 83p.

- McAuliffe, C.D., 1987. Organism exposure to volatile/soluble hydrocarbons from crude oil spills – a field and laboratory comparison. In: *Proceedings of the 1987 International Oil Spill Conference*, American Petroleum Institute, Washington, D.C., pp. 275-288.
- Moum, J.N., W.D. Smyth, 2001. Upper ocean mixing processes. *Encyclopedia of Ocean Sciences*, Academic Press, pp. 3093-3100.
- National Research Council (NRC), 2005. Understanding Oil Spill Dispersants: Efficacy and Effects. National Research Council, Ocean Studies Board, National Academies Press, Washington, DC.
- Ohlmann, J.C., P. White, L. Washburn, E. Terrill, B. Emery, and M. Otero, 2007. Interpretation of Coastal HF Radar-Derived Surface Currents with High-Resolution Drifter Data. *Journal of Atmospheric and Oceanic Technology*, 24, pp. 666-680.
- Okubo, A., 1971. Oceanic Diffusion Diagrams. *Deep-Sea Research* 8, pp. 789-802.
- Okubo, A. and R.V. Ozmidov, 1970. Empirical Dependence of the Coefficient of Horizontal Turbulent Diffusion in the Ocean on the Scale of the Phenomenon in Question. *Atmospheric and Ocean Physics* 6(5), pp. 534-536.
- Payne, J.R., E. Terrill, M. Carter, M. Otero, W. Middleton, A. Chen, D. French-McCay, C. Mueller, K. Jayko, W. Nordhausen, R. Lewis, M. Lampinen, T. Evans, C. Ohlmann, G.L. Via, H. Ruiz-Santana, M. Maly, B. Willoughby, C. Varela, P. Lynch and P. Sanchez, 2007a. Evaluation of Field-Collected Drifter and Subsurface Fluorescein Dye Concentration Data and Comparisons to High Frequency Radar Surface Current Mapping Data for Dispersed Oil Transport Modeling. In: *Proceedings of the Thirtieth Arctic and Marine Oil Spill Program (AMOP) Technical Seminar*, Emergencies Science Division, Environment Canada, Ottawa, ON, pp. 681-711.
- Payne, J.R., D. French-McCay, C. Mueller, K. Jayko, B. Longval, M. Schroeder, E. Terrill, M. Carter, M. Otero, S.Y. Kim, W. Middleton, A. Chen, W. Nordhausen, R. Lewis, M. Lampinen, T. Evans, and C. Ohlmann, 2007b. *Evaluation of Field-Collected Drifter and In Situ Fluorescence Data Measuring Subsurface Dye Plume Advection/Dispersion and Comparisons to High-Frequency Radar-Observation System Data for Dispersed Oil Transport Modeling*, Draft Final Report 06-084, Coastal Response Research Center, NOAA/University of New Hampshire, Durham, NH, 98 p. plus 8 appendices. Available at <http://www.crrc.unh.edu/>.
- Reed, M., O. Johansen, P.J. Brandvik, P. Daling, A. Lewis, R. Fiocco, D. Mackay, and R. Prentki, 1999. Oil Spill Modeling Towards the Close of the 20th Century: Overview of the State-of-the-Art. *Spill Science and Technology Bulletin*, 5 (1), pp. 3-16.
- Reed, M., P.S. Daling, O.G. Brakstd, I. Singsaas, L.-G. Faksness, B. Hetland, and N. Efrøl, 2000. OSCAR 2000: A Multi-Component 3-Dimensional Oil Spill Contingency and Response Model. In: *Proceedings of the 23rd Arctic Marine Oilspill Program (AMOP) Technical Seminar*, Environment Canada, Ottawa, Ontario, pp. 663-952.
- Smith, J.A., 1992. Observed Growth of Langmuir Circulation. *Journal of Geophysical Research*, 97, 5651-5664.

- Spaulding, M.L., S.B. Saila, E. Lorda, H.A. Walker, E.L. Anderson and J.C. Swanson, 1983. Oil Spill Fishery Interaction Modelling: Application to Selected Georges Bank fish Species. *Estuarine, Coastal and Shelf Science*, 16, pp. 511-541.
- Spaulding, M.L. , 1988. A State-of-the-Art Review of Oil Spill Trajectory and Fate Modeling. *Oil and Chemical Pollution*, 4, pp. 39-55.
- Thorpe, S.A., 1995. Dynamical processes at the sea surface. *Progress in Oceanography*, 35, pp. 315-352.
- Thorpe, S.A., 2000. Langmuir Circulation and the Dispersion of Oil Spills in Shallow Seas. *Spill Science and Technology Bulletin*, 6(3), pp. 213-223.
- U. S. Coast Guard (USCG), 1999. *Response Plan Equipment Caps Review: Are Changes to Current Mechanical Recovery, Dispersant, and In Situ Burn Equipment Requirements Practicable?* Washington, D.C., United States Coast Guard, U. S. Department of Transportation, pp. 1-177, plus appendices.
- Youssef, M., 1973. The Behavior of the Near Ocean Surface Under the Combined Action of Waves and Currents in Shallow Water. PhD Dissertation, Department of Ocean Engineering, University of Rhode Island, Narragansett, RI, 212 p.
- Youssef, M. and M. L. Spaulding, 1993. Drift Current Under the Action of Wind Waves. In: *Proceedings of the Sixteenth Arctic and Marine Oilspill Program Technical Seminar*, Ottawa, ON, Canada, pp. 587-615.
- Youssef, M. and M.L. Spaulding, 1994. Drift Current Under the Combined Action of Wind and Waves in Shallow Water. In: *Proceedings of the Seventeenth Arctic and Marine Oilspill Program (AMOP) Technical Seminar*, Ottawa, ON, Canada, pp. 767-784.

Table 1. Wind and wave conditions, mixed layer depth, water density, and stability characteristics.

Date	8 Nov 2005	21 Mar 2006	22 Mar 2006	21 Jun 2006	22 Jun 2006	1 Nov 2006	2 Nov 2006
Wind direction (deg., from) at LJPC1	191	284	319	256	249	325	327
Wind speed (m/s) at LJPC1	5.7	5.0	4.2	3.5	3.3	5.2	4.2
Mixed layer depth (m)	9	12	15	10	7	11	8
Dye plume penetration depth (m)	10	10*	10 to 14	6	7	10**	8

* Plume measured for approximately one hour and dye may not have reached maximum depth during sampling.

** Deepest depth sampled but dye is known to have gone deeper since the edge of the plume was not detected at that depth (Fluorescence was still above background at 10 m.)

Table 2. Estimates of horizontal dispersion coefficients (D_x) derived from dimensions of the dye in images over time (based on linear regression).

Date	8 Nov 2005*	21 Mar 2006	22 Mar 2006	21 Jun 2006	22 Jun 2006	1 Nov 2006	2 Nov 2006
Downwind axis: D_x (m^2/s)	0.46	1.46	0.60	51.46	12.34	10.44	25.08
Downwind axis: Correlation (r^2)	0.965	0.876	0.970	0.936	0.932	0.973	0.926
Downwind axis: # observations	3	26	18	29	7	39	31
Crosswind axis: D_x (m^2/s)	-0.29	0.57	0.15	5.01	0.82	0.68	2.37
Crosswind axis: Correlation (r^2)	0.606	0.773	0.275	0.936	0.963	0.692	0.933
Crosswind axis: # observations	3	27	21	28	11	41	31
Radial spread: D_x (m^2/s)	0.01	1.01	0.45	17.32	4.19	3.17	8.27
Radial spread: Correlation (r^2)	0.002	0.966	0.930	0.959	0.954	0.960	0.946
Radial spread: # observations	3	23	17	28	7	39	31

* The results for this date are not reliable because of the limited number of observations and short time period of photographic observations.

Table 3. Estimates of vertical (D_z) dispersion coefficients based on vertical profiles of dye concentration. [Note the units here are cm^2/s , while the values of D_x in Table 6 are in m^2/s .]

Date	8 Nov 2005	21 Mar 2006	22 Mar 2006	21 Jun 2006	22 Jun 2006	1 Nov 2006	2 Nov 2006
Dz mean (cm^2/s)	16	30	6	6	8	10	11
Dz std dev (cm^2/s)	12	6	5	9	8	4	11
# observations	4	2	11	14	13	27	25

Table 4. Decline of vertical (D_z) dispersion coefficients over time (fit to equation 5, and predicted D_z using equation 6) in the 1 and 2 November 2006 experiments.

Parameter	1 Nov 2006	2 Nov 2006
slope (m in equation 5)	0.753	0.282
Intercept ($\log(a)$, equation 5)	-1.780	-0.158
Correlation (r^2)	0.837	0.437
a (equation 5)	0.017	0.696
D_z at 5min	12.9	10.0
D_z at 1 hrs	8.3	2.8
D_z at 2 hrs	7.0	1.7

Table 5. Equivalent volume, area and diameter of 100% mortality if oil of the indicated volume were dispersed into a surface mixed layer 8m deep.

Volume of Oil	Impact Measure	21 Mar 2006	22 Mar 2006	21 Jun 2006	22 Jun 2006	1 Nov 2006	2 Nov 2006
170 m^3	Equivalent volume (millions of m^3)	1.1	1.2	2.3	6.3	2.2	2.1
	Equivalent area (km^2)	0.13	0.15	0.29	0.79	0.28	0.26
	Diameter of equivalent area (m)	412	439	606	1005	597	580
38 m^3	Equivalent volume (millions of m^3)	0.13	0.17	0.13	0.83	0.15	0.17
	Equivalent area (km^2)	0.016	0.021	0.016	0.104	0.019	0.021
	Diameter of equivalent area (m)	144	163	142	364	154	164

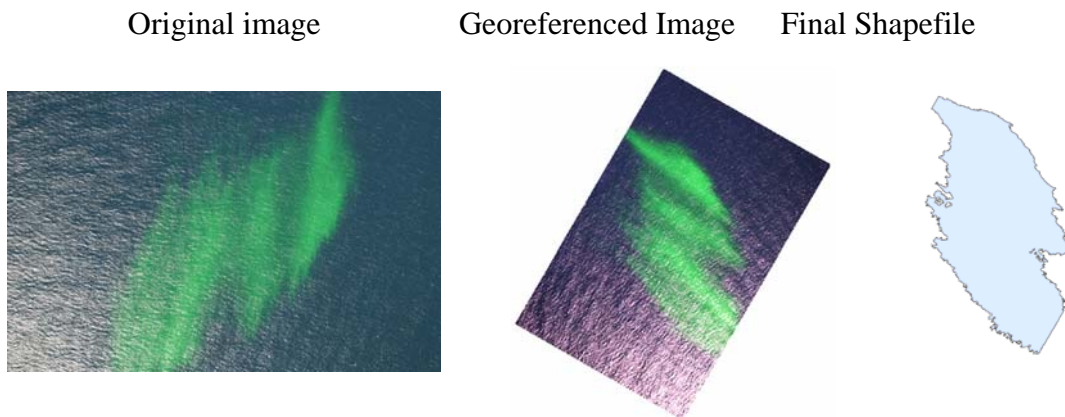


Figure 1. Aerial photograph processing steps.

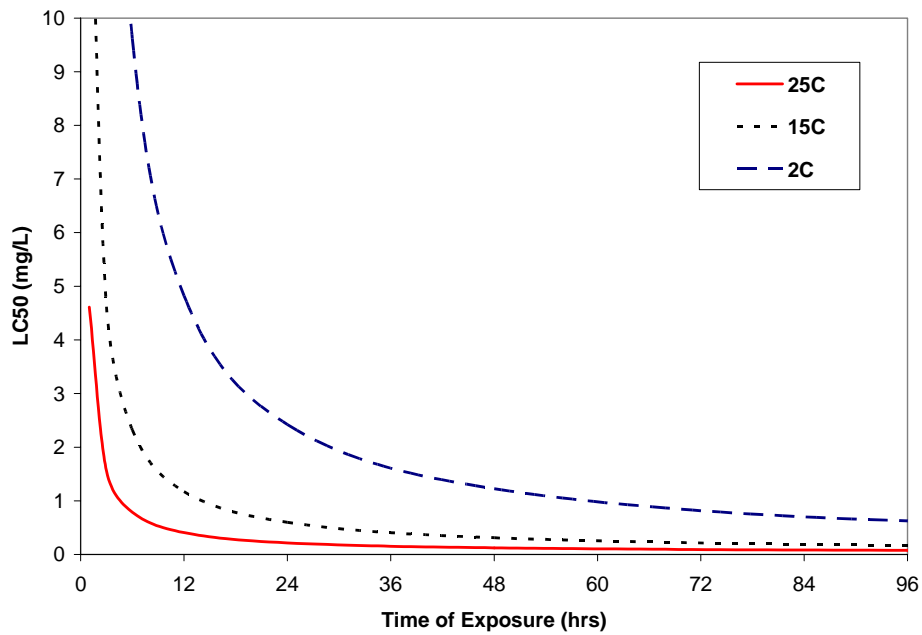


Figure 2. LC50 of dissolved PAH mixtures from oil, as a function of exposure duration and temperature.

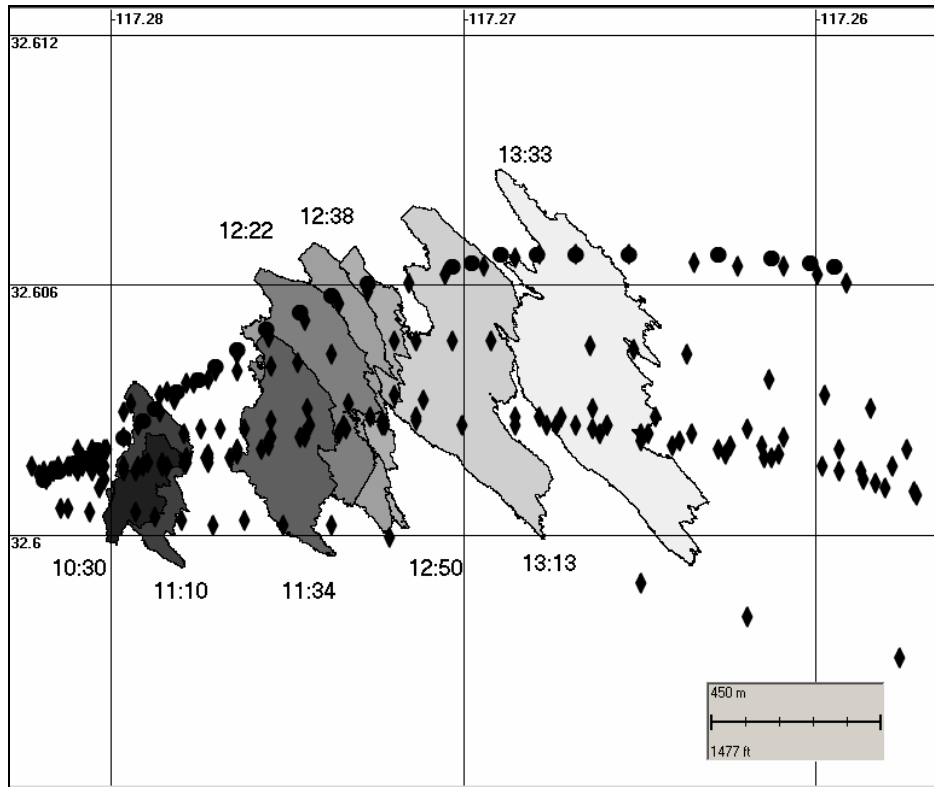


Figure 3. Dye plume dimensions and movements over time and drifter tracks for the 22 March 2006 experiment (diamonds for drogues at 1m, circles for drogues at 5m).

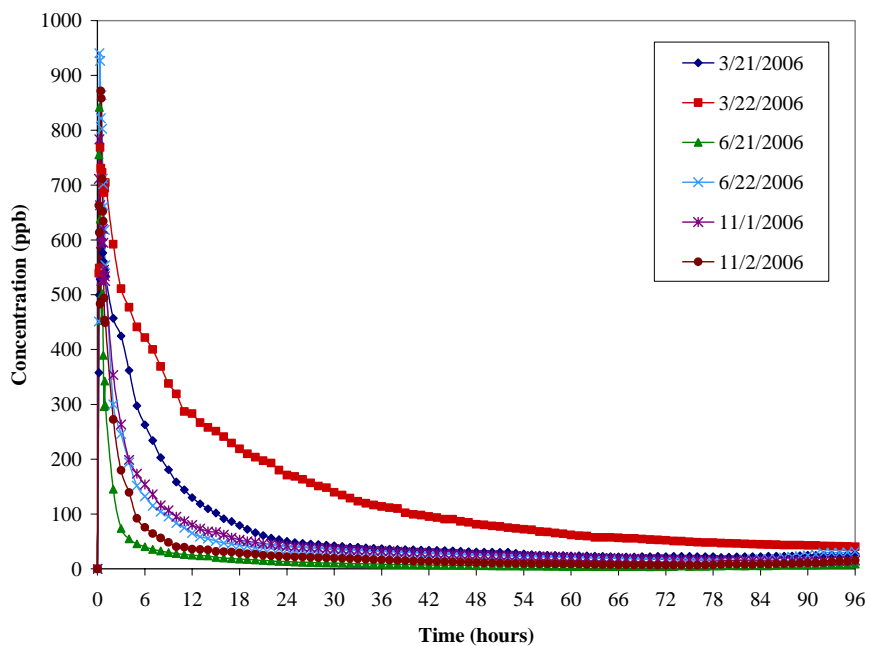


Figure 4. Maximum dissolved aromatic concentration in the center of the plume versus time after dispersion of 170 m³ of oil under environmental conditions on the indicated dates.

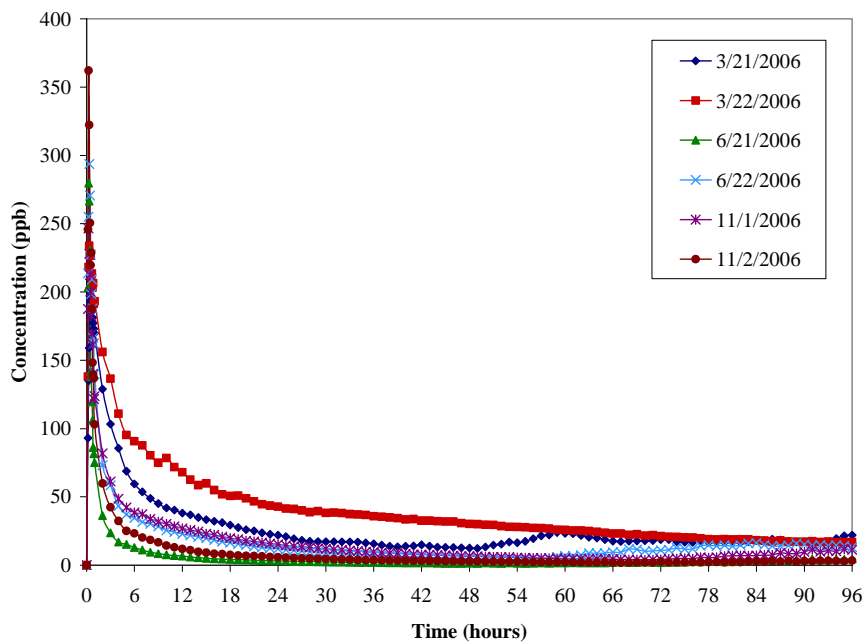


Figure 5. Maximum dissolved aromatic concentration in the center of the plume versus time after dispersion of 38 m³ of oil under environmental conditions on the indicated dates.